Original Paper

Landslides (2013) 10:611–622
DOI 10.1007/s10346-012-0347-3
Received: 12 January 2012
Accepted: 6 July 2012
Published online: 31 July 2012

Matteo Mantovani · Stefano Devoto · Emanuele Forte · Arianna Mocnik · Alessandro Pasuto · Daniela Piacentini · Mauro Soldati

A multidisciplinary approach for rock spreading and block sliding investigation in the north-western coast of Malta

Abstract Landslides are widespread along the north-western coast of the Island of Malta and are strictly linked to the structural setting. Exemplary cases of rock spreading and block sliding phenomena characterise this stretch of coast. They are favoured by the overposition of two different geological units widely outcropping there, the Blue Clay Formation and the Upper Coralline Limestone Formation. The latter forms a wide plateau, bordered by vertical cliffs. At the foot of the cliffs, clayey terrains crop out and develop gentle slopes covered by large blocks detached and moved by rock spreading and block sliding phenomena. These mass movements are favoured by the fragile behaviour of limestones, which cap clays, otherwise characterised by visco-plastic properties. In order to investigate the kinematics and the evolution of these types of coastal landslides, a multidisciplinary and multitechnical approach was applied on a study site, named Il-Prajjet, which provides a spectacular case of rock spreading evolving into block sliding. This paper illustrates the results achieved by means of different engineering geological and geophysical techniques allied with traditional detailed geomorphological survey and mapping. In particular, the surface displacements of the landslides were determined using long-term GPS observations, acquired approximately every 6 months, over a 4.5-year period. A network of GPS benchmarks were distributed on the edge of a limestone plateau affected by rock spreading and on a series of displaced blocks making up a large block slide, finally enabling the definition of the state of activity and the rates of movement to be performed. In addition, the results deriving from two continuous fissurimeters more recently installed at the edge of two persistent joints over the block sliding area are outlined, with reference to the correlation between variations of crack apertures and precipitation input. In order to identify main structural discontinuities and to reconstruct variability of underground surface contact between clays and overlying limestones, Resistivity Tomography profiles and GPR investigations were carried out. Finally, the results obtained by combining the outputs of geophysical surveys and different field monitoring activities can be considered a first step on which numerical models can be developed and validated, in order to assess landslide hazard and risk of this stretch of Maltese coastline.

Keywords Rock spreading · Block sliding · Multidisciplinary approach · Monitoring · Malta

Introduction

Recently, due to frequent disasters, the interest in slope failures has enhanced significantly and the consciousness that environmental protection should take place through a deep knowledge of the natural processes has significantly increased. However, some types of landslides, such as lateral spreading, are not generally considered as hazardous phenomena due to their very slow evolution. In most cases, the investigation of lateral spreading has been limited to a pure descriptive geomorphological approach without a consistent long-term monitoring support aiming at the understanding of their triggering mechanisms and kinematics.

Lateral spreading processes consist of an extension of a fragile rock mass over a softer underlying material, characterised by a displacement along an undefined basal shear surface (Pasuto and Soldati 1996). Despite their slow speed rates, these phenomena may cause damage to human structures and favour or trigger collateral faster movements such as falls, topples, slides and flows (Soldati and Pasuto 1991). For these reasons, a quantitative interpretation of lateral spreading evolution and its relationships with collateral landslides are fundamental in terms of risk assessment and possible mitigation strategies (e.g. Vlcko 2004).

The north-western coast of Malta can be considered as an open-air laboratory for the study of lateral spreading phenomena, namely rock spreading, due to the peculiar geological-geomorphological setting related to the presence of extensional faults and to the overposition of rock masses characterised by different geomechanical properties.

The study area, named Il-Prajjet, is located in the northern part of a cove at the head of Anchor Bay (Fig. 1). The location exhibits some of the most remarkable geomorphological features related to slope failures and provides an impressive example of rock spreading evolving into a large block slide (Magri et al. 2008; Devoto et al. 2012). Moreover, risk issues are involved because of the presence of an amusement park.

This study illustrates the application of a multidisciplinary and multitechnical approach aiming at defining quantitatively the kinematics of the above-mentioned rock spreading and block sliding phenomena, by combining the results of detailed geomorphological survey and mapping with monitoring surveys and geophysical investigations. As regards the latter, Electrical Resistivity Tomography (ERT) profiles were employed to identify large-scale lithological contacts, to highlight the tectonic structures and to assist the geomorphological interpretation. The orientation, persistency and width of the discontinuity sets of calcareous rock masses have been reconstructed by means of a Ground Penetrating Radar (GPR) campaign. A Global Positioning System (GPS) network has been operative since October 2006 (Magri et al. 2007, 2008; Magri 2009) and so far ten surveys have been carried out allowing us to measure the intensity and the direction of the displacement vectors and thus inferring the kinematics of the on-going processes. In order to understand possible triggering factors (e.g., rainfall input) of the instability phenomenon, more recently two automated fissurimeters were installed to monitor continuously two persistent open fractures in the block sliding area. Moreover, possible correlations of the evolution of the whole instability phenomenon with precipitations and earthquakes have

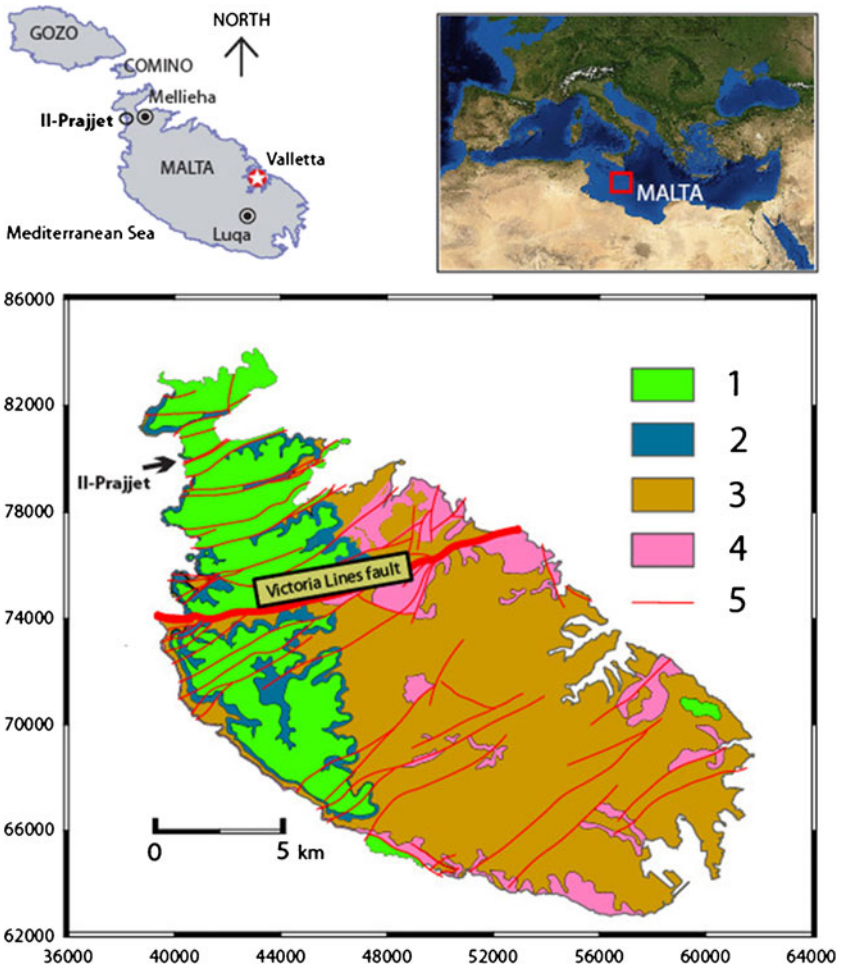

Fig. 1 Location of the study area of Il-Prajjet and geological sketch map of the Island of Malta (adapted from Pedley et al. 2002). *1* Upper Coralline Limestone Formation, *2* Blue Clay Formation, *3* Globigerina Limestone Formation, *4* Lower Coralline Limestone Formation and *5* Fault

been assessed. The results achieved allowed a deeper understanding of the lateral spreading phenomenon at Il-Prajjet to be carried out that is essential in order to forecast the slope instability evolution, making possible a reliable hazard assessment.

Geological and structural setting

Excluding limited Quaternary deposits, the Island of Malta is composed of sedimentary rocks such as limestones, marls and clays, Upper Oligocene–Upper Miocene in age (Pedley 1978; Pedley et al. 2002). The older geological unit is the Lower Coralline Limestone Formation, which is composed by a massive grey limestone, underlying the yellowish Globigerina Limestone Formation that conversely, is made up by a fine grained limestone which represents the most extensive outcropping lithology in the Island of Malta. The stratigraphic sequence continues with the more erodible Blue Clay Formation, which is mainly composed by marls and clayey terrains, and ends-up with the Upper Coralline Limestone Formation. The latter two geological formations are dominant in the northern part of Malta.

Pedley (1978) subdivided the Upper Coralline Limestone in members, basing on lithology and on the recognition of faunal population. Indeed, from a geomechanical viewpoint, Upper and Lower Coralline Limestone formations are very similar, except for the presence of a thick yellowish member in the lower portion of the upper formation, named Mtarfa Member, which is a bioclastic limestone mainly made up by algal rhodolite beds and echinoid fragments. Mtarfa Member is hence characterised by low values of uniaxial rock strengths and is highly jointed, compared with the uppermost members included onto Upper Coralline Limestone Formation. Along the north-western coast, Mtarfa member outcrops widely along the basal part of structural cliffs (Oil Exploration Directorate 1993).

From a tectonic viewpoint, the central sector of Malta is crossed by an impressive tectonic discontinuity, the Victoria Lines fault, which structurally divides the Island in two portions (Fig. 1). North of the fault, in proximity of the study area, the structural setting is characterised by a horst–graben system, which deeply influences the topography displacing the entire coastline (Alexander 1988; Said and Schembri 2010) and also controls the development of lateral spreading phenomena.

Grabens correspond to valleys, which cross Malta approximately with a WSW-ENE direction, flanked by a series of parallel plateaus (horsts), which are bordered by sub-vertical slopes. For this reason, the coastline is irregular, with alternated cliffs and lowland coasts. Horsts form vertical plunging cliffs whereas lowland coasts occur where coastlines intersect

the above-mentioned structural depressions, forming coves such as Anchor Bay (Devoto et al. 2012).

Climatic setting

The climate of the Maltese archipelago is typically Mediterranean with hot and dry summers, relatively wet autumns and winters, short and mild winters.

The average annual temperature is 18 °C and the monthly averages range from 13 (end of January) to 27 °C (August). The highest temperatures are reached in August and July, which are characterised by extremely scarce precipitations (Fig. 2a).

Winter seasons show only rare occurrences of cold weather generally brought by north and north-eastern winds from central Europe. At least 70 % of the average annual precipitation occurs during October to January period, mostly related to thunderstorms. Rainfall distribution is slightly higher on the northern portion of the Island of Malta, where the cold Mistral wind blows more frequently. The storms often involve enough precipitation to cause floods in low-lying areas and landslides along the coastal cliffs.

Malta receives on average 550 mm of precipitation annually, but rainfall varies significantly from year to year. The longest rainfall dataset available is related to the station of Luqa and is provided by the Malta Meteorological Office since 1929 (Fig. 2b). The wettest year occurred in 1951 with 956 mm, whereas 1947 was the driest year with only 227 mm. With reference to the last decade, notable variations were recorded and it seems that drought and wet years alternate regularly: 2001 was the driest year with 338 mm while 2003 was the wettest with 899 mm.

In order to investigate the correlation between precipitation and landslide activity, meteorological data recorded by Mellieha weather station (active since 2003) were collected and analysed. The station is located about 2 km east from Il-Prajjet.

The study area

The study area of Il-Prajjet is situated at the head of Anchor Bay, which is a small embayment along the north-western coast of Malta. The geomorphological evolution of this sector of the Island is deeply controlled by a linkage of different factors such as tectonics, lithology and landslides, which make up a predominant feature in the area.

The semi-elliptical shape of the bay is related to the presence of relevant faults, oriented E-W near the coastline and ENE-WSW along the valley. On the north side of the bay, Blue Clay Formation

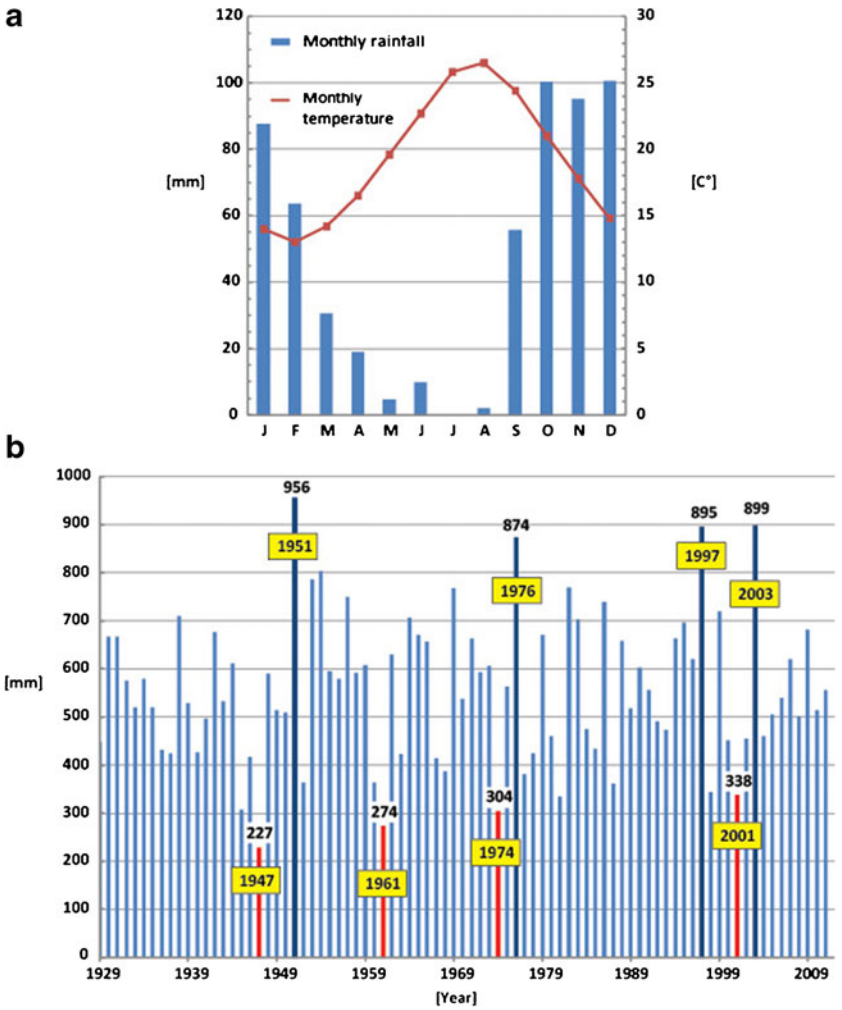

Fig. 2 Rainfall and temperature distribution in the Island of Malta: **a** climatograph constructed by averaging monthly rainfall data recorded since 2003 and temperature data available since 2007 at the Mellieha meteorological station. **b** Historic record of annual rainfall at Luqa weather station from 1929 to 2011

and Upper Coralline Limestone Formation outcrop and their superimposition favours the development of an impressive rock spreading phenomenon, which has evolved into a large block slide affecting the entire north-eastern sector of the cove, where an amusement park is located (Fig. 3).

The rock spread affects the limestone plateau, which is limited by a structural cliff 15–20 m high, oriented approximately parallel to the coast. The deformation, which occurred along tectonic discontinuities, has further jointed the rock mass, which is now characterised by persistent fissures and cracks, reaching 150 m of length.

The joint system also favours karst processes (Paskoff and Sanlaville 1978), which have a prominent role in the gravitational processes as well. Precipitation percolates from the limestone plateau along the vertical cracks forming a suspended aquifer at the sub-horizontal contact between impermeable clayey terrains and overlying permeable limestones (Mangion 1991). At the bottom of the cliff, the block sliding area consisting of eight large limestone boulders (with volumes varying from 70 up to a maximum of 13,350 m^3) is clearly observable. The above-mentioned boulders were detached and moved from the edge of the plateau, as a consequence of rock masses isolation by persistent structural discontinuities, opened and enlarged by rock spreading phenomena. Conversely, the southern part of Anchor Bay is characterised by vertical Upper Coralline Limestone cliffs which directly reach the sea. The absence of outcrops of clays prevents the occurrence of lateral spreading phenomena on this side of the bay.

Methods

A multidisciplinary approach is of paramount importance in the study of complex coastal instability processes that are usually triggered and governed by multiple factors. Contemporary application of different methodologies and techniques allows data cross-check, validation and a reliable interpretation to be performed. This approach can also assist in the identification of the most effective techniques to investigate single parameters in terms of reliability, resolution and accuracy.

The study area of Il-Prajjet has been investigated combining detailed geomorphological mapping with geophysical surveys and landslide monitoring (Fig. 4).

Geological and geomorphological field surveys provided a clear picture of the distribution and evolution of the geomorphic processes, landforms and relationships with tectonic structures. They were also relevant for defining the type of monitoring, equipment and techniques to be used and for outlining the sites to be monitored. Geophysical investigations were integrated with geomorphological and engineering-geological analyses to better determine the characteristics of the terrains affected by rock spreading and block sliding, including the definition of volumes involved in the mass movement process, the geometry of the sliding surface and the role of groundwater (e.g. Bogoslovsky and Ogilvy 1977; Gallipoli et al. 2000; Bichler et al. 2004; Göktürkler et al. 2008). Two geophysical surveys were carried out at Anchor Bay. In detail, ERT was performed along the valley that develops inland from the bay in order to obtain information on a wider area about the main tectonic elements related to landslide occurrence and evolution. High-resolution GPR surveys were conducted over the larger blocks making up the block sliding area (Fig. 4), with the aim of identifying the stratigraphic contacts and assessing the degree of fracturing.

The monitoring system used to detect the surface displacements in the rock spreading and block sliding areas consists of a nine benchmarks GPS network (including the reference point) and of two automated fissurimeters. Three GPS benchmarks were installed in the rock spreading area (see points 101 to 103 in Fig. 8), corresponding to the limestone plateau, whereas the other five (points 104 to 108) and the fissurimeters were positioned in the block sliding area (Fig. 5).

The GPS technique has already been proved as a powerful tool in ground deformation analysis. Several papers dealing

Fig. 3 Rock spreading and block sliding phenomena occurring on the northern side of Anchor Bay

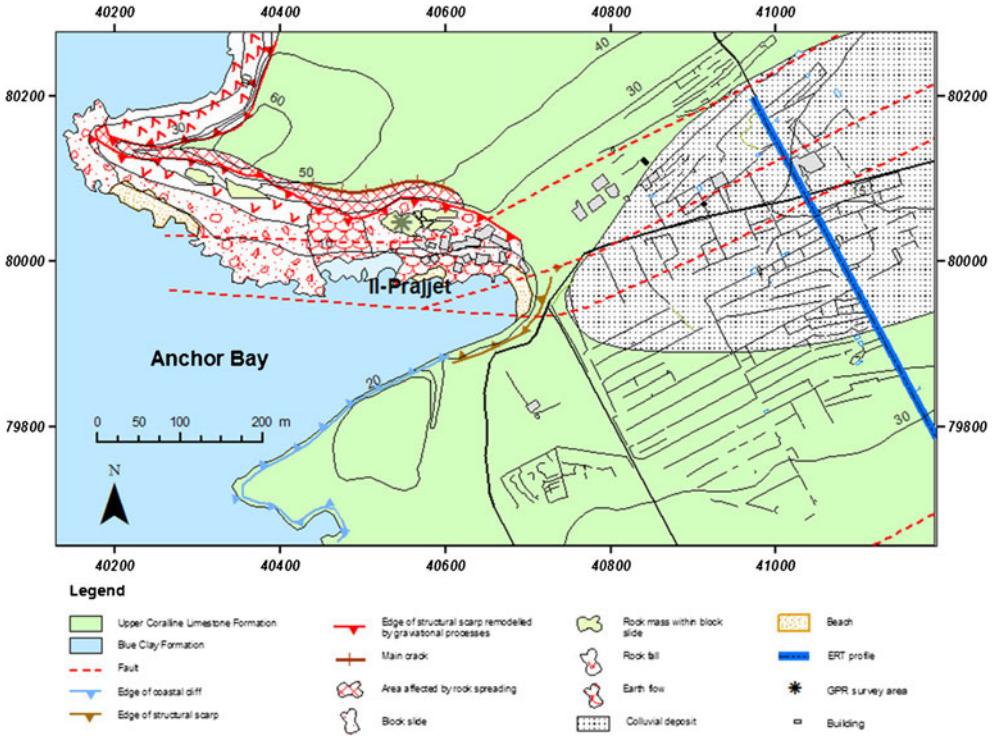

Fig. 4 Geomorphological sketch map of the study area and location of geophysical surveys

with landslides monitoring (Gili et al. 2000; Coe et al. 2003; Corsini et al. 2005; Brückl et al. 2006) showed the capability of GPS to measure displacement with high accuracy and reliability. For this reason, a GPS network was installed in October 2006 at Il Prajjet. Since then ten surveys were carried out, twice per year, in spring at the end of the wet season, and in autumn at the end of the dry season. Since the deformations were expected to be very slow, an additional care was used in the definition and planning of the survey procedures, so that the highest possible accuracy could be achieved. In order to guarantee the repetitiveness, avoiding positioning errors, a simple forced centring device for the GPS antenna was realised at each benchmark consisting in cylindrical steel rods with a diameter of 1 cm and 10 cm long, drilled into the rocks for a depth of about half their length.

The fissurimeters installed in the block sliding area consist of a titanium rod fixed at two cardan joint drilled on the edges of a fracture. The displacements are measured by a potentiometer that converts the electric signal sent by the transducer and record it in a 12-bit data logger. The instruments were set to make a measurement every 6 h. Displacement data acquisition started at the end of March 2010.

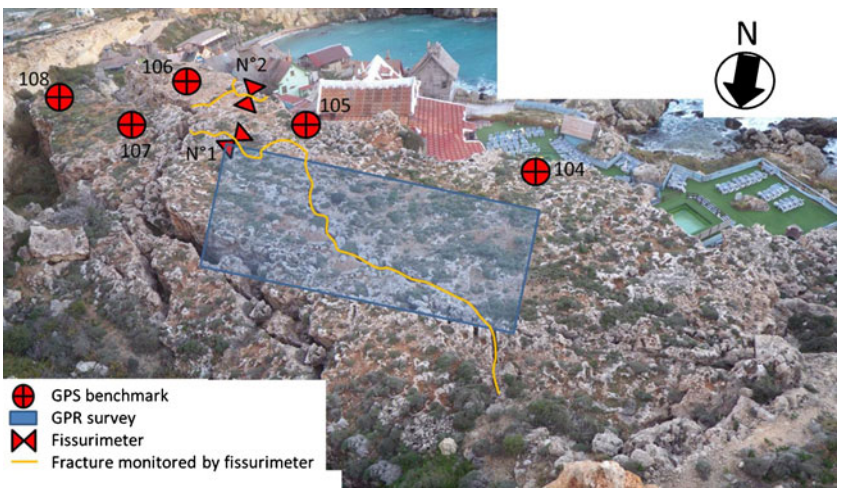

Fig. 5 Location of GPS benchmarks, fissurimeters and GPR survey over the block sliding area

Geophysical data collection, processing and interpretation

ERT surveys encompassed two-dimensional (2D) profiles east of Il-Prajjet (see Fig. 4), obtained with a Syscal Pro multi channel resistivity meter developed by IRIS Instruments and equipped with 48 metallic electrodes. Various electrode geometries have been tested (Wenner, Wenner–Schlumberger and Dipole–Dipole) as far as various electrode spacing (range from 5 up to 10 m). The use of different electrode configurations is essential since both vertical and lateral resolutions are very important for the study area. In fact, vertical resolution allows to highlight lithological contacts and internal layering (and can be achieved especially using the Wenner geometry), while lateral variations related to tectonic or weathering phenomena can be better imaged using Dipole–Dipole acquisition schemes.

GPR data were acquired on the block sliding area using a GPR Zond equipped with 300 and 500 MHz shielded antennas (Figs. 4 and 5). In order to obtain a precise imaging of the rock mass and mainly to reconstruct the three-dimensional (3D) discontinuity network, dense acquisition grids were focused on the larger blocks. The trace distance was fixed within the range 2.5–10 cm, while the profile spacing was 0.5 or 1 m. This technique allows obtaining pseudo-3D (or 2.5) datasets with high lateral resolution, which is fundamental for a detailed rock mass characterisation (Grasmueck 1996; Grasmueck et al. 2003; Heincke 2006; McClymont et al. 2010).

ERT analysis recorded low resistivity values (less than 100 Ωm) in the shallower part (maximum 6 m in depth), higher values within the range 100–2,500 Ωm for a variable depth and a very low resistivity (below 100 Ωm with local minimum of few ohm metres) in the deepest part. With the longer electrode combination tested (460 m between the current and potential electrodes), a maximum penetration depth of about 80 m was achieved. The apparent resistivity data were inverted taking into account the topography using RES2DINV software (Loke and Barker 1996), which applies a smoothness-constrained least-squares inversion algorithm to produce a 2D true resistivity model. All the acquired data were edited before inversion process in order to eliminate suspicious, noisy and out-of-range spikes. Figure 6 provides the ERT inverted profile acquired across the valley before (A) and after interpretation (B). The results of the tomography are quite representative of the situation of the entire north-western coast of Malta where the limestone outcrops, except along the axis of the valleys, which are instead filled by soils and colluvial sediments. The thickness does not exceed 5–6 m (horizon S in Fig. 7) and therefore can only be partially identified on ERT measurements with large electrode spacing (in the reported example the minimum distance between current and potential electrodes centres is equal to 20 m). The calcareous rocks show a resistivity between 100 and 2,000 Ωm. This range is quite large and shifted to relative low values as compared with limestone resistivities from literature (e.g. Reynolds 1997). This behaviour can be explained considering that in the study area there are several different rocks roughly described as "limestones" but including cross-stratified grainstones, channelled packstones, pure carbonate mudstones and also carbonate sandstones (wackes) (Pedley et al. 2002). Moreover, the carbonates contain a discontinuous, but important, suspended aquifer locally exploited for agricultural uses (Mangion 1991). In the deepest part of the ERT, the resistivity decreases reaching values below 20 Ωm (below L-C contact on Fig. 6): these materials can be interpreted as the Blue Clay Formation. Since the resistivity below the mean sea level (dashed black line on Fig. 6) does not show any significant variation, no apparent salt intrusions are thought to be present. From the profile of Fig. 6, it is also apparent that not only sub-horizontal contacts but also clear sub-vertical structures (f1 and f2) are present. These zones show low resistivity within relative narrow areas (10 to 15 m wide), without significant vertical changes and can be interpreted as fault zones and related to the regional horst-and-graben setting. We correlated these faults with those observed on the plunging cliff at the Anchor Bay. The attitude of the southern fault changes from 275/65° just above the beach within the bay, to ENE/sub-vertical into the valley.

Single 2D GPR profiles were analysed in order to extract information both about the shallow limestone stratigraphy and the landslide related discontinuities of the blocks in the sliding area. Both standard and specific processing procedures including 2D and 3D attributes analyses (instantaneous attributes, coherency measurements, spectral decomposition, texture attributes) were applied to the GPR measurements, with the aim of extracting all the information embedded within the data and hardly accessible especially on low signal-to-noise-ratio environments. These techniques are well known for reflection seismic analysis (e.g. Chopra and Marfurt 2007) and, due to the well-demonstrated similarities between the kinematic properties of seismic and GPR data, in recent years the attributes have been tested on GPR data with the necessary adjustments (Sénéchal et al. 2000; Corbeanu et al. 2002; McClymont et al. 2008; Forte et al. 2010, 2012). Single 2D profiles (Fig. 7a) and the entire volume obtained combining all the sections acquired along a dense (in the present case 0.5 by 0.5 m) grid were processed and analysed (Fig. 7b). Depth conversion of GPR data (from the Two Way Traveltime traces originally recorded) was achieved integrating the velocity analysis obtained by fitting of selected diffraction hyperbolas on GPR profiles (for a general description of this processing procedure see e.g. Jol 2009; for a case history related to limestone investigation see e.g. Pipan et al. 2003) with direct correlations with the outcrops. The shallower portion of the 2D sections shows reflective layered materials interpreted as compact limestone (layered limestones (LL)). Below this unit there are low reflective materials up to a clear wavy high-amplitude reflection (LC) that probably are massive carbonates almost transparent from the EM point of view. This is in well agreement with the typical stratigraphic column characterised by laminated soft limestones (Mtarfa Member) overlying the Blue Clay Formation. The LC reflection can be observed at different depths within all the explored volume (22 m by 7 m). Figure 7b shows the geometrical reconstruction of this contact and of the bottom limit of LL. The latter is almost parallel to the topographic surface with a more or less constant depth of about 4.5 m, while the LC contact has a dip toward S-SE. Considering both the stratigraphic sequence of the area and the GPR signature, this level can be interpreted as the contact between carbonates and the Blue Clay Formation, which is responsible of the diffused spreading and sliding phenomena. The GPR volume interpretation permits to deduce all the geometrical parameter (attitude) of this surface with a detail level comparable to the information measured

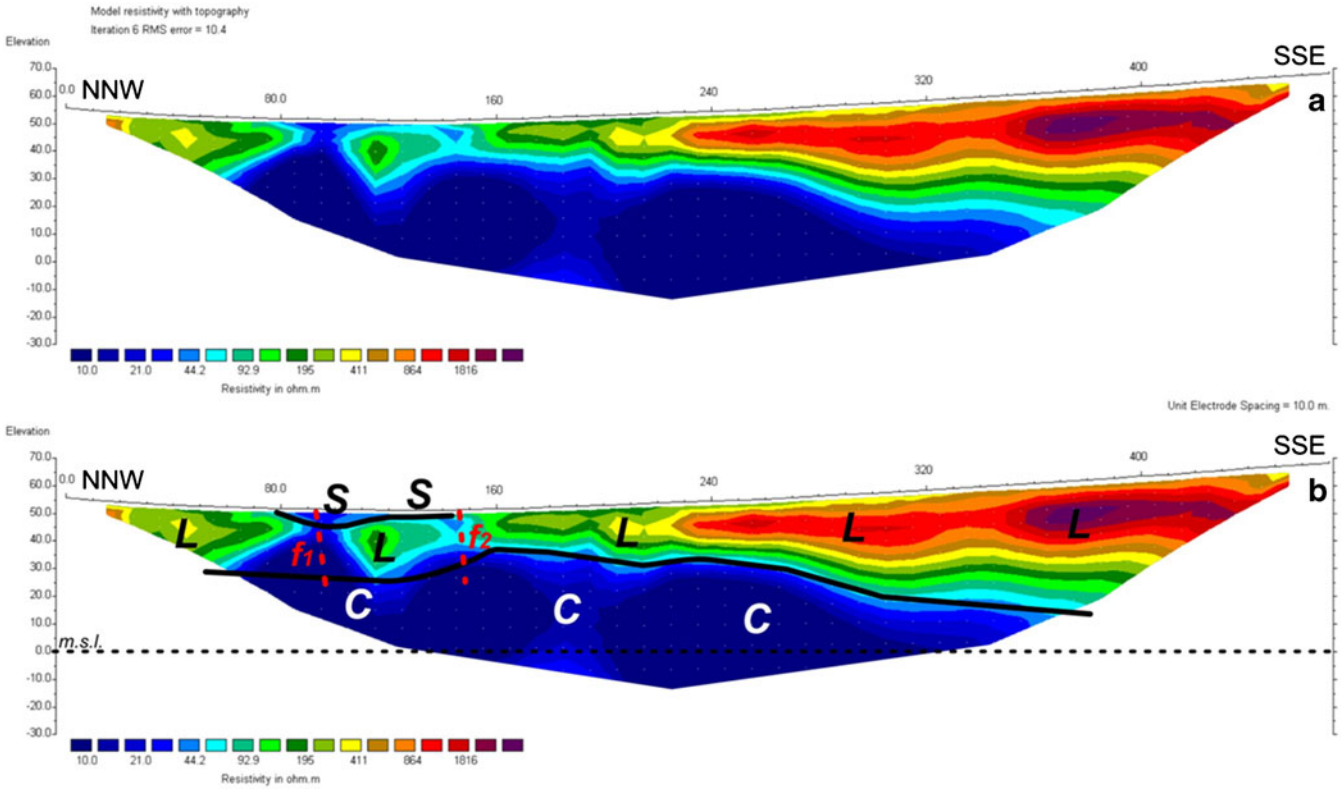

Fig. 6 Inverted ERT (**a**) with interpretation superimposed (**b**). *S* surface soil and colluvial sediments, *L* limestone, *C* clay. *f1* and *f2* mark two important fault zones. *Vertical* and *horizontal scales* are equal

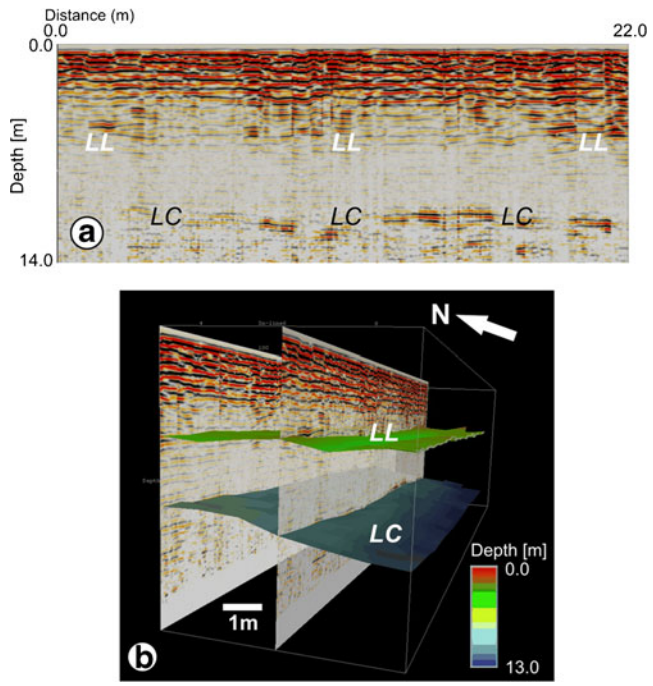

Fig. 7 2D 300 MHz GPR profile (*inline*) taken from the dense grid of 22 by 7 m (**a**). Two inlines from 3D data volumes with the interpreted layered limestone bottom (*LL*) and the inferred contact between limestone and the underlying sediments of the Blue Clay Formation (*LC*). The *colour bar* shows the depth below the topographic surface (**b**)

on free faces and outcrops. The strike of this lithological contact is 230° and the mean dip close to 16°.

Monitoring system: data collection and interpretation

Two SR530 Leica Geosystems GPS receivers capable to track the L1 C/A code and L2 P code on 24 channels were used to detect displacements over the rock spreading and block sliding areas (Fig. 8). The static relative positioning technique was employed: one receiver was placed over the reference point (master), located in a stable area located S-E of Il-Prajjet, and the other was moved around the eight benchmarks located over the rock spreading and block sliding area. The distance among the reference point and the farthest benchmark (103) is 357 m. The acquisition time was set in 20 min with a 2-s sampling rate with a cut off angle of 15°. The data were stored and post-processed using precise ephemeris in order to determine with highest accuracy achievable the baseline between each point. The displacements caused by the lateral spreading phenomena have been determined comparing differences in the baselines among the reference station and the benchmarks through the different surveys. The cumulated displacements recorded from October 2006 to March 2011 are expressed by the red arrows and the circles in Fig. 8 (planar and vertical components, respectively).

In the rock spreading area, points 102 and 103 recorded a vertical deformation of 6.3 and 10.9 cm, respectively, which is higher than the planar one, ranging from 3.3 to 2.9 cm. Benchmark 101 shows a different trend of movement with a planar component of 3.4 cm and a non-significant vertical displacement. If benchmark 101, that is placed over an isolated rock mass, is disregarded

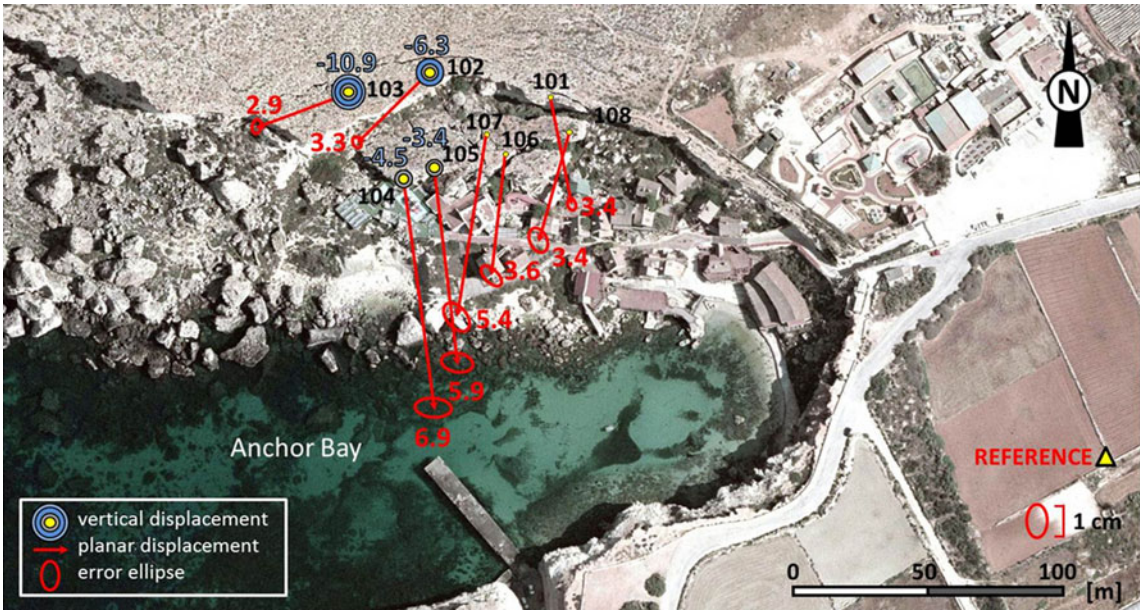

Fig. 8 Cumulated displacement vectors of the GPS network recorded between October 2006 and March 2011 at Il-Prajjet. Benchmarks 101, 102 and 103 are located in the rock spreading area while points 104, 105, 106, 107 and 108 are placed some 15 m below on the block sliding area. Deformation values are expressed in centimetres

and only the displacement pattern recorded at points 102 and 103 is taken into account, we can assume that the rock spreading area has also subsided during the investigated period. This displacement pattern may indicate that rock spreading is accompanied by an incipient block sliding in the upper part of the cliff.

On the other hand, the benchmarks located on the block sliding area (104 to 108) recorded planar displacements ranging from 3.4 to 6.9 cm and, with the exception of 104 and 105, no significant lowering was detected. This shows a prevailing planar displacement, including block tilting that can be related to the ongoing block sliding process.

The module of the 3D deformation vector recorded by each benchmark has been plotted in function of the time in Fig. 9. During a 4.5-year investigation period, all the GPS benchmarks showed an almost constant deformation rate whose estimated values are reported in Table 1.

Since 2010 GPS monitoring was accompanied by measurements performed by means of two fissurimeters which monitor two persistent cracks located in between the most active sliding blocks (where GPS benchmarks 104 and 105 are positioned, see Fig. 5). The deformation data, superimposed to the daily rainfall heights, recorded by the meteorological station of Mellieha have been plotted in Fig. 10.

Fissurimeter No. 1 went out of scale from the 16th of September 2010 until the 14th of November of the same year (see horizontal green line on Fig. 10) due to an excessive reduction of the aperture of the monitored crack. In order to avoid a similar problem the instrument was readjusted and the data acquired since then rescaled to preserve homogeneity with those collected before. Although the deformations recorded are extremely small, a correlation with daily rainfall can be noticed (see yellow arrows in Fig. 10 highlighting the major events). The narrowing of the fracture is evident during the wet season while its reopening starts a while after the precipitations have decreased.

Discussion of results

The multi-technical investigation carried out at Il-Prajjet has provided relevant information for better understanding the kinematics of the ongoing displacements and for defining the characteristics of the materials involved.

The detailed geomorphological survey enabled the recognition and mapping of the morphological features of the coastal instability phenomenon affecting the area of Il-Prajjet and to relate them with the structural setting of the site. The geomorphological investigation showed that the upper part of Il-Prajjet is characterised by rock spreading phenomena whilst the lowered blocks were interpreted as part of a block slide (Fig. 4).

The inverted ERT data showed that there are at least two direct faults along the axis of the valley bordering toward south the study area (Fig. 6). This structural setting justifies the presence of lateral spreading phenomena on the north side of Anchor Bay and its absence on the south.

Using GPR data collected from the block sliding area (Fig. 5), we imaged: a high-reflective zone interpreted as layered limestones; a semi-transparent portion interpreted as massive limestone (probably related to the Mtarfa Member of the Upper Coralline Formation); and a high-attenuating area interpreted as the contact between limestones and clayey terrains. This contact, having a mean inferred strike of 230° and dip close to 16°, conditions the evolution of block movements within the sliding area. There is in fact a good agreement with the direction of the displacement vectors toward S-SE, recorded by GPS benchmarks 104 and 105 (see Fig. 8). In other words, the blocks in the sliding area move along the ruling gradient of the lithological contact dip that does not necessarily correspond to the direction of the maximum steepness of the clayey slopes.

Extremely high correlation values with the linear regression lines interpolating the displacement values obtained by means of GPS are found for all the benchmarks analysed (see Fig. 9)

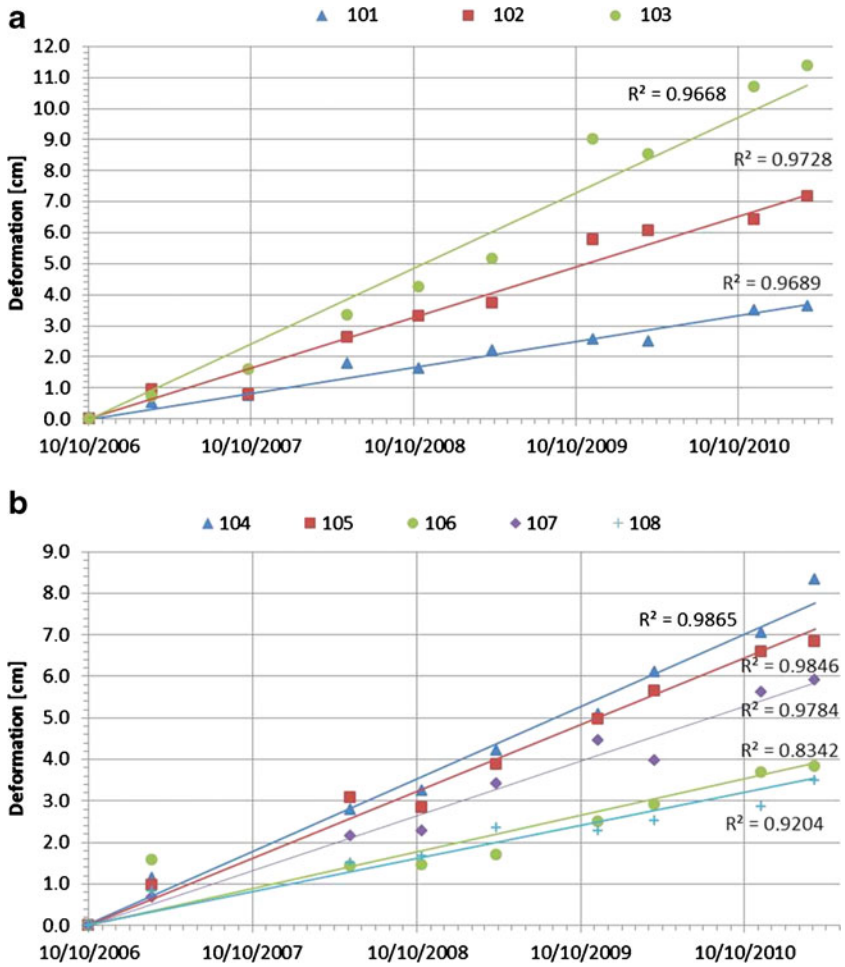

Fig. 9 Trend of the 3D deformation recorded by the GPS benchmark over the rock spreading area (**a**) and over the block sliding area (**b**) reconstructed from linear regression lines. R^2 is the correlation coefficient

witnessing a constant rate of deformation of the blocks involved in the process.

Through the fissurimeter data analyses, it was possible to interpret the short-time scale kinematics of the limestone blocks making up the block sliding area. Fissurimeter n°1 seems to be highly influenced by precipitation. A clear deformation started exactly in correspondence with the first significant rain (22.8 mm on 10th of September, see Fig. 10) after the dry season and continued with another large fracture narrowing, few days later, in correlation with a rainfall of 55.8 mm (see yellow arrows in Fig. 10). This event is the second larger rainfall measured by the Mellieha meteorological station in 2010 and was responsible to the out-of-scale of the instrument. Due to this faulty operation, other correlations between deformations and the main rainfall events until the 14th of November cannot be highlighted. A second significant narrowing of the fracture started on the 2nd of January 2011 in correspondence with a 16.6 mm rainfall and continued until the complete end of the rainfall events at the end of March.

Table 1 Estimated values of the constant deformation rates retrieved by the angular coefficient of the interpolating regression lines for each GPS benchmark

Benchmark	Deformation rate (cm/year)	Benchmark	Deformation rate (cm/year)
101	0.8	105	1.6
102	1.6	106	0.9
103	2.4	107	1.3
104	1.8	108	0.8

The relationship between the mineralogy content of the Maltese clays and their geotechnical properties and behaviour has been analysed in detail by Dykes (2002). In his work, their high smectite content (approximately 40 %) is significant as the structure of the clay mineral can incorporate, or loose, water depending on overall moisture status of the clay material, the effect of which is to cause the material to swell on wetting or shrink on drying.

For this reason, as described in Fig. 11, the closing of the fracture measured by fissurimeter No. 1 can be explained with the swelling of the underlying clays, that settle the inclination of the blocks. Conversely, the reopening of the fracture is related to the shrinking of clayey levels during drier periods.

This interpretation is in agreement with the non-significant variations recorded by fissurimeter No. 2 which is

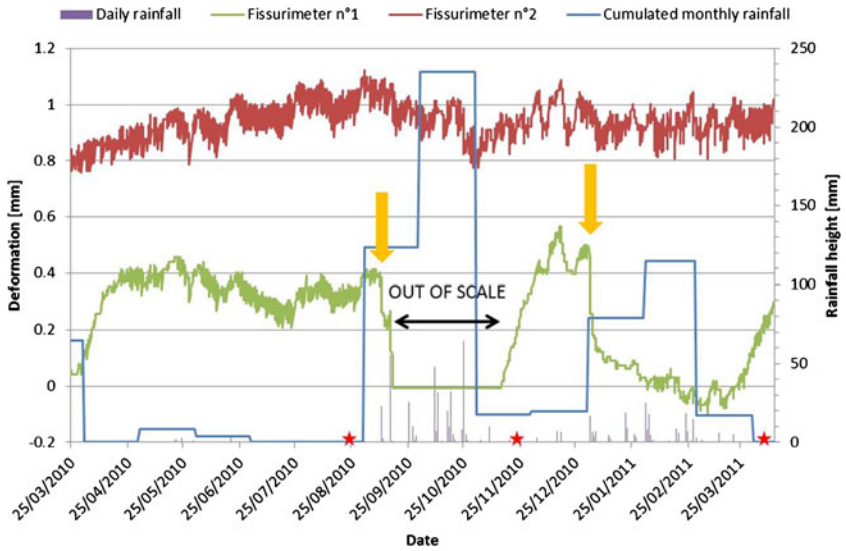

Fig. 10 Deformations measured by the fissurimeters plotted with the daily and the monthly cumulated rainfall recorded by the meteorological station of Mellieha. Zero reading for fissurimeter No. 1 and 2 was set respectively to 0.0425 and 0.8180 mm. *Yellow arrows* highlight the beginning of the two major events recorded; *red stars* are located in correspondence of earthquakes

aiming at measuring the displacements of a marginal block which is largely detached from the surrounding blocks and does not lay over the clays. No correlation with the rainfall heights can, in this case, be outlined. Since the fracture preserved its original width during the observation period, we also can assume that the block does not show a single displacement but it moves together with the adjacent blocks where GPS benchmarks 104 and 105 are located.

With respect to the triggering factors that might cause deformation or displacement, we also investigated the possible influence of earthquakes. First, we selected from the public catalogue "ISIDE" of the Italian and Mediterranean earthquakes, implemented and updated by INGV (website: http://iside.rm.ingv.it/iside), all the events occurred when the fissurimeters were working (25th March 2010–14th April 2011) and having the epicentre near the Maltese archipelago, i.e. within the latitude range between 35° and 37° and the longitude between 13° and 16°. Forty events with magnitude Richter of ≥2 (maximum magnitude equals to 3.8 Richter) were recorded during that period. The Peak Ground Acceleration (PGA) calculated for the M 3.8 event, having the epicentre about 102 km from the study area, and for the closest one (M=2.4; distance, 6.5 km) are 0.12 and 0.48 cm/s^2, respectively. These values have been obtained using the mean attenuation function proposed by Moratto et al. (2009) and disregarding any site effect. The maximum PGA value inferred from earthquakes occurred during the period monitored by fissurimeters reached a value of 1.13 cm/s^2 and refers to a M 3.0 event with epicentre at about 11 km from the study area, occurred the 19th November 2010.

We also considered the PGA due to strong events (M>4) having epicentre quite far from the Island of Malta (M=6.1, on 01/04/2011, 1100 km; M=5.6, on 22/08/2010, 550 km). The maximum PGA was reached by the latter event with a value of 0.9 cm/s^2. This is just a first order approximation of the acceleration occurred on the study area, which is however very low. In fact, no correlations were detected between seismic activity and the displacements recorded (see Fig. 10).

Hence we tested another approach and proceeded the other way round. We extracted from the records of the fissurimeters the date and time of the most significant displacements and looked for possible seismic events occurred at that time. We found two relatively important deformations (about 0.3 mm) on 15th of September 2010 and 1st of January 2011 (see Fig. 10). However, no significant earthquakes were recorded on these dates.

In detail: 16 earthquakes with magnitude of >2.0 were recorded with maximum magnitude of 3.9 on 16th September 2010 and epicentre very far at about 1,100 km from the study area. We can conclude that at least for the period of continuous monitoring by means of fissurimeters, no seismic event showed any correlation with deformations.

Conclusions

The multisciplinary and multitechnical approach used to study the coastal instability of a stretch along the north-west coastline of Malta has proved to be effective for a better understanding of the causes, mechanisms, state of activity and evolution of a complex mass movement, which displays rock spreading and block sliding phenomena. Through the use of geophysical investigation techniques and a deformation monitoring network, we were able to assist geological and geomorphological interpretation of the instability phenomena affecting the area of Il-Prajjet. This integrated approach allowed us to operate at both spatial and temporal scales.

The research showed that, especially in such instability context, geophysical investigations are an essential tool since they provide the means to recognise the position and the orientation of structural elements, even when masked by shallow sediments. Both field observations performed on rock outcrops and ERT data confirmed the presence of direct high-angle faults crossing Anchor Bay.

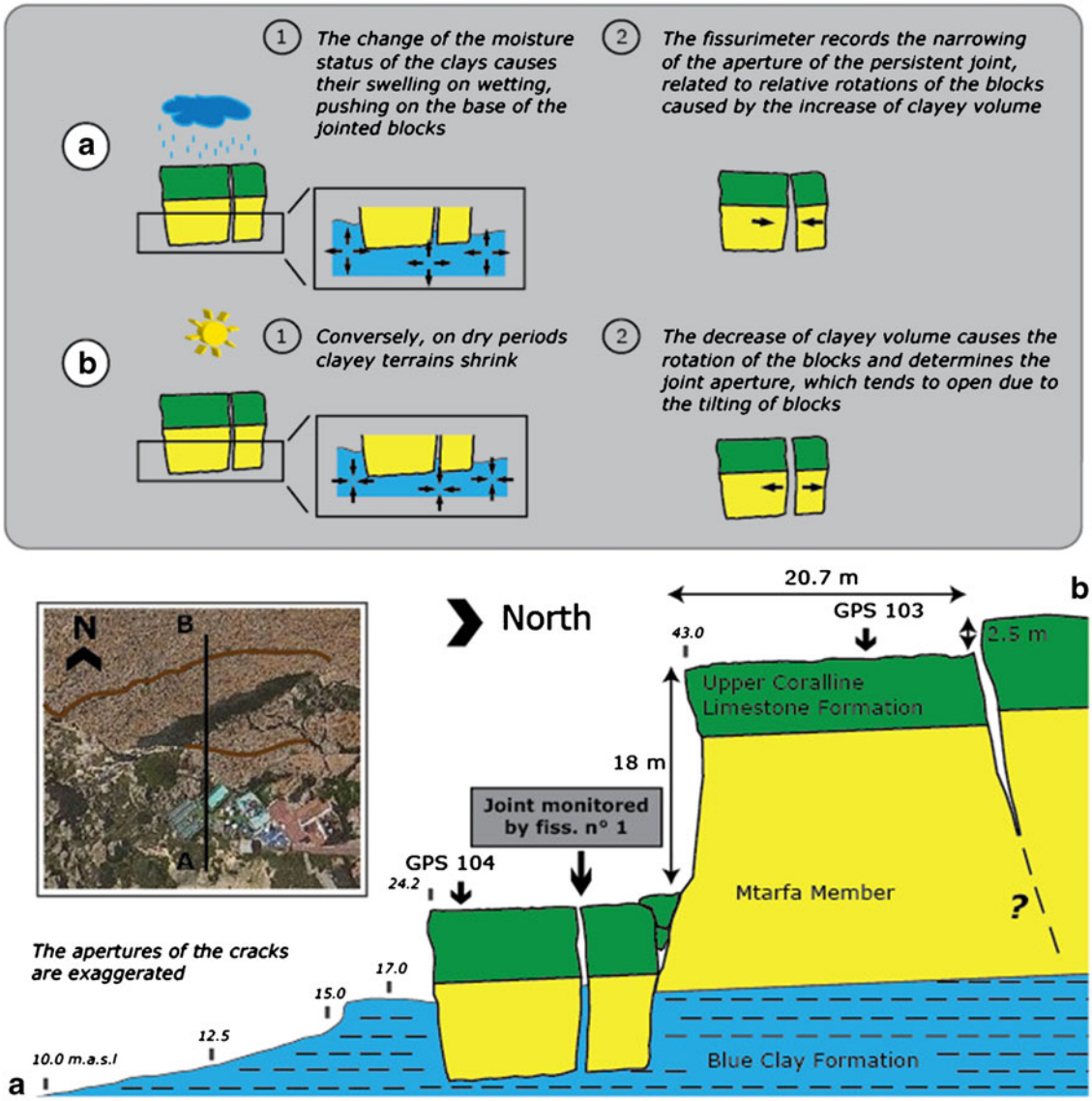

Fig. 11 Geological section through the unstable area of Il-Prajjet and description of swelling and shrinking processes affecting the block sliding area as a result of wetting and drying of clayey terrains

GPS data showed that both the rock spread and block slide processes recognised at Il-Prajjet are active and that the rate of deformation is higher than expected (up to 2.7 cm/year). GPS monitoring also highlighted that over the 4.5 years of data collection, the displacements were characterised by linear trends.

Moreover, the comparison of deformation data and geophysical investigations conducted at a more detailed scale by means of GPR analysis enabled us to reconstruct the kinematics and the geometry of the limestone blocks, which make up the block sliding area at Il-Prajjet.

With a sampling rate of 6 h the fissurimeters provided important information on the kinematic behaviour in a short temporal scale. The data collected during more than 1 year suggest that the dislocated blocks in the block sliding area move as a rigid unit and that the opening of fractures are linked to the alternation of wet and dry periods. The analysis of rainfall inputs and displacements trend showed that the aperture of the monitored fracture tend to narrow during rainy periods, whereas it tends to widen during drier periods. This behaviour is probably related to the swelling and shrinking of the clays below the limestones (see Fig. 11). This differential settling can produce secondary fractures within the main limestone blocks, possibly increasing the probability of rock falling from the edge of the limestone cliffs. On the other hand, no specific correlations were found between block displacement and seismic events recorded during the fissurimeter monitoring period.

The overall results obtained make up a sound basis for further research activities which may include the development and validation of numerical models, in order to assess landslide hazard and risk along this stretch of the north-western coast of the Island of Malta.

Acknowledgements

The research activities were funded by the EUR-OPA Major Hazards Agreement of the Council of Europe through the European Centre on Geomorphological Hazards (CERG) and the Euro-Mediterranean Centre on Insular Coastal Dynamics (ICoD) in the frame of the projects "Coastline at risk: methods for multi-hazard assessment" and "Coupling terrestrial and marine datasets for coastal hazard assessment and risk reduction in changing environments". The authors are grateful to Dr. Alan Dykes for his precious suggestions and gratefully acknowledge the support of Halliburton through the University of Trieste Landmark academic grant.

References

Alexander D (1988) A review of the physical geography of Malta and its significance for the tectonic geomorphology. Quat Sci Rev 7:41–53

Bichler A, Bobrowsky P, Best M, Douma M, Hunter J, Calvert T, Burns R (2004) Three-dimensional mapping of a landslide using a multi-geophysical approach: the Quesnel Forks landslide. Landslides 1:29–40

Bogoslovsky VA, Ogilvy AA (1977) Geophysical methods for the investigation of landslides. Geophysics 42:562–571

Brückl E, Brunner FK, Kraus K (2006) Kinematics of a deep-seated landslide derived from photogrammetric, GPS and geophysical data. Eng Geol 88:149–159

Chopra S, Marfurt KJ (2007) Seismic attributes for prospect identification and reservoir characterization. SEG/EAGE editions, Tulsa

Coe JA, Ellis WL, Godt JW, Savage WZ, Savage JE, Michael JA, Kibler JD, Powers PS, Lidke DJ, Debray S (2003) Seasonal movement of the Slumgullion landslide determined from global positioning system surveys and field instrumentation, July 1998–March 2002. Eng Geol 68(1–2):67–101

Corbeanu R, McMechan GA, Szerbiak RB, Soegaard K (2002) Prediction of 3-D fluid permeability and mudstone distributions from Ground Penetrating Radar (GPR) attributes: example from the Cretaceous Ferron sandstone member, east-central Utah. Geophysics 67(5):1495–1504

Corsini A, Pasuto A, Soldati M, Zannoni A (2005) Field monitoring of the Corvara landslide (Dolomites, Italy) and its relevance for hazard assessment. Geomorphology 66(1–4):149–165

Devoto S, Biolchi S, Bruschi VM, Furlani S, Mantovani M, Piacentini D, Pasuto A, Soldati M (2012) Geomorphological map of the NW Coast of the Island of Malta (Mediterranean Sea). J Maps 8(1):33–40

Dykes AP (2002) Mass movements and conservation management in Malta. J Environ Manage 66:77–89

Forte E, Di Cuia R, Casabianca D, Pipan M, Riva A (2010) 3D stratigraphic and tectonic reservoir analogue studies with integrated GPR data: an example from a limestone quarry. In: Proceedings of the XIII International Conference on Ground Penetrating Radar, GPR, Lecce, Italy, 21–25 June 2010

Forte E, Pipan M, Casabianca D, Di Cuia R, Riva A (2012) Imaging and characterization of a carbonate hydrocarbon reservoir analogue using GPR attributes. J Appl Geophys 81:76–87

Gallipoli MR, Lapenna V, Lorenzo P, Mucciarelli M, Perrone A, Piscitelli S, Sdao F (2000) Comparison of geological and geophysical prospecting techniques in the study of a landslides in southern Italy. Eur J Environ Eng Geophys 4:117–128

Gili JA, Corominas J, Rius J (2000) Using global positioning system techniques in landslide monitoring. Eng Geol 55:167–192

Göktürkler G, Balkaya Ç, Erhan Z (2008) Geophysical investigation of a landslide: the Altindağ landslide site, İzmir (western Turkey). J Appl Geophys 65:84–96

Grasmueck M (1996) 3-D ground-penetrating radar applied to fracture imaging in gneiss. Geophysics 61(4):1050–1064

Grasmueck M, Weger R, Horstmeyer H (2003) How dense is dense enough for a 'real' 3D GPR survey? SEG Tech Prog Expanded Abstr 22(1):1180–1183

Heincke B (2006) Acquisition and processing strategies for 3D georadar surveying a region characterized by rugged topography. Geophysics 70:K53–K61

Jol HM (ed) (2009) Ground Penetrating Radar: Theory and Applications. Elsevier, Amsterdam. ISBN: 978-0-444-53348-7, p. 524

Loke MH, Barker RD (1996) Rapid least-squares inversion of apparent resistivity pseudosections using a quasi-Newton method. Geophys Prospect 44:131–152

Magri O (2009) Investigation of landslides along the North-West coast of Malta and related hazard issues. Ph.D. thesis, University of Modena and Reggio Emilia, Italy

Magri O, Mantovani M, Pasuto A, Soldati M (2007) Monitoring the state of activity of lateral spreading phenomena along the north-west coast of Malta using the GPS technique. Analele Universitatii Din Oradea 17:5–10

Magri O, Mantovani M, Pasuto A, Soldati M (2008) Geomorphological investigation and monitoring of lateral spreading along the north-west coast of Malta. Geogr Fis Dinam Quat 31:171-180

Mangion M (1991) Impact of geological structural features on the hydrology and hydrogeology of Malta. Bachelor thesis. Master's thesis, University of Malta

McClymont AF, Green AG, Streich R, Horstmeyer H, Tronicke J, Nobes DC, Pettinga J, Campbell J, Langridge R (2008) Visualization of active faults using geometric attributes of 3D GPR data: an example from the Alpine fault zone, New Zealand. Geophysics 73(2):B11–B23

McClymont AF, Green AG, Kaiser A, Horstmeyer H, Langridge R (2010) Shallow fault segmentation of the Alpine fault zone, New Zealand revealed from 2-D and 3-D GPR surveying. J Appl Geophys 70(4):343–354

Moratto L, Costa G, Suhadolc P (2009) Real-time generation of shake maps in the southeastern Alps. Bull Seismol Soc Am 99(4):2489–2501

Oil Exploration Directorate (1993) Geological map of the Maltese Islands. Office of the Prime Minister, Valletta

Paskoff R, Sanlaville P (1978) Observations géomorphologiques sur les côtes de l'archipel Maltais. Z Geomorphol 22:310–328

Pasuto A, Soldati M (1996) Landslide recognition: Identification, movement and causes, chapter rock spreading. Wiley, Chichester, pp 122–136

Pedley M (1978) A new lithostratigraphical and palaeoenvironmental interpretation for the coralline limestone formations (Miocene) of the Maltese Islands. Overseas Geol Miner Resour 54:273–291

Pedley M, Hughes Clarke M, Galea P (2002) Limestone Isles in a Crystal Sea: the geology of the Maltese Islands. Publishers Enterprises Group, Malta

Pipan M, Forte E, Guangyou F, Finetti I (2003) High resolution GPR imaging and joint characterization in limestone. Near Surf Geophys 1:39–55

Reynolds JM (1997) An introduction to applied and environmental geophysics. Wiley, Chichester

Said G, Schembri J (2010) Malta, pages 751–759. In: Bird ECF (ed) Encyclopedia of the worlds coastal landforms volume 1. Springer, Dordrecht

Sénéchal P, Perroud H, Sénéchal G (2000) Interpretation of reflection attributes in a 3-D GPR survey at Valle d'Ossau, western Pyrenees, France. Geophysics 65 (5):1435–1445

Soldati M, Pasuto A (1991) Some cases of deep-seated gravitational deformations in the area of Cortina d'Ampezzo (Dolomites). Implications in environmental risk assessment. In: M. Panizza, M. Soldati, M.M. Coltellacci (eds.) European Experimental Course on Applied Geomorphology, vol. 2, Istituto di Geologia Università degli Studi, Modena, pp. 91–104

Vlcko J (2004) Extremely slow slope movements influencing the stability of Spis Castle, UNESCO site. Landslides 1:67–71

M. Mantovani (✉) · A. Pasuto
Research Institute for Geo-hydrological Protection,
CNR-IRPI. National Research Council of Italy,
Corso Stati Uniti 4, 35127, Padua, Italy
e-mail: matteo.mantovani@irpi.cnr.it

S. Devoto · D. Piacentini · M. Soldati
Department of Chemical and Geological Sciences,
University of Modena and Reggio Emilia,
Largo S. Eufemia 19, 41121, Modena, Italy

E. Forte · A. Mocnik
Department of Mathematics and Geosciences,
University of Trieste,
Via E. Weiss 1, 34128, Trieste, Italy